

MHD-Control of a Shock Wave Structure at a Hypersonic Flow

V. M. Fomin, V. P. Fomichev** and M. A. Yadrenkin****

** Khristianovich Institute of Theoretical and Applied Mechanics , Russia
fomin@itam.nsc.ru*

*** Khristianovich Institute of Theoretical and Applied Mechanics , Russia
fomin@itam.nsc.ru*

**** Khristianovich Institute of Theoretical and Applied Mechanics , Russia
yadrenkin@itam.nsc.ru*

Abstract

The present paper devoted to the experimental studies of MHD flow control of a hypersonic air flow with external ionization created by the pulse and radiofrequency (RF) discharges. MHD-interaction localized on a flat plate in a hypersonic flow has been considered. It has been shown experimentally that both the pulse and the RF discharge can be efficiency used for the flow ionization in the transverse B-field and for the generation of the nonequilibrium conductivity. The MHD-interaction permits to control the shock wave structure of the flow and generate control forces and moments on the surface streamlined at test conditions.

1. Introduction

There are reasons to believe that at present an advance of hypersonic flights to the mesosphere is one of the directions of the aerospace science development. It seems to be possible to fly at these altitudes with the speed higher than 2500 – 3500 m/s at certain conditions. The high velocities create the preconditions for using of magnetohydrodynamic techniques of flow control at low magnetic induction (less than 1 T). Magnetoplasdynamic (MHD) effect on the air flow around bodies at hypersonic flight conditions permits to change a shock wave structure of the flow significantly. MHD-interaction localized on a flat plate in a hypersonic air flow has been considered at present paper.

2. Test rig and techniques

Currently, the experimental researches of hypersonic flows under the conditions approaching the full-scale parameters are performed in hot-shot wind tunnels. Experimental studies have been carried out at MHD test rig based on a shock tube in ITAM [1]. Gas heated by reflected shock wave in a settling chamber accelerates up to $M = 6, 8, 10$ in the wind tunnel nozzle. Cross section of the flow is round with diameter 105 mm. The test rig allows to simulate a hypersonic flow, which is typical for the flight altitude of 30 – 50 km with $M = 6, 8, 10$. The test section is placed in the electromagnet, which creates a uniform magnetic field up to 2.3 T. Schematic of the MHD test rig is presented in Figure 1. Typical gas-dynamic parameters of the simulated airflow are shown in Table 1. Experimental results with $M = 6, 8$ are presented in the work.

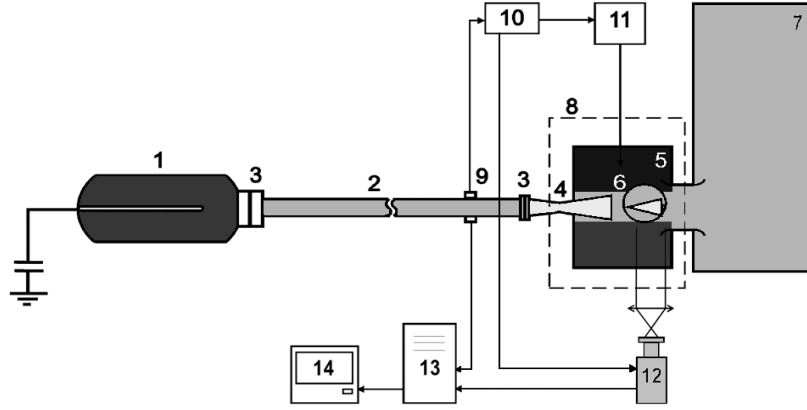


Figure1: Test rig scheme. 1-high-pressure chamber, 2-shock tube channel, 3-membrane, 4-conical nozzle, 5-test section, 6- device of external ionization, 7- receiver, 8-magnetic system, 9-gauge, 10-amplifier-generator, 11-ionizer power supply, 12-CCD-camera, 13-computer, 14-monitor

Table 1: Gas-dynamic parameters of the airflow simulated on the test rig

| Mach number | Flow rate, m s^{-1} | Static pressure, Tor | Flow density, kg m^{-3} | Flow temperature, K |
|-------------|------------------------------|----------------------|----------------------------------|---------------------|
| 6 | 1 900 | 12 | 5 | 270 |
| 8 | 1 950 | 2 | 0.1 | 150 |
| 10 | 2 000 | 0.5 | 2.5×10^{-3} | 100 |

Following parameters are measured in each experiment to investigate the MHD-interaction:

- Shock wave parameters,
- Gas parameters in the nozzle prechamber,
- Parameters of ionizing discharge,
- MHD-interaction parameters.

Optical visualization of the oblique shock wave generated by the model is also used as a method of the study.

P_0 and T_0 , parameters in the nozzle prechamber, have been defined by measurements of pressure in the prechamber using a piezoelectric transducer and the calculated speed of the shock wave in the channel of the shock wind tunnel. Operating characteristics of the pre-ionizers are defined by measurements of the current and voltage of the discharge. The current is measured with the help of high-frequency transformers of the current; the voltage is measured using a voltage divisor with an induction - output signal.

MHD - interaction parameters are defined using the value of the total current measured in the zone of interaction and voltage on MHD-electrodes. The total current is measured using current transformers, the voltage is measured using a voltage divisor with an inductive connection to an oscillograph. All the measurements of the electrical parameters are implemented using the current transformers, which allow performing the signal transmission to oscillograph without a galvanic coupling in the range of frequency from 100 Hz up to 10^7 Hz.

Changing of the shock wave structure has been visualized by shadow technique based on AVT [2] (adaptive visualizing transparency). Synchronization of operation of all blocks and measurement system is in the range of 1 μs . Accuracy of measurements is determined by accuracy of electronic devices and gauges, used in tests (piezoelectric transducers and current transformers), this error is less than 5-10 %.

3. Pulse and RF discharges for the ionization of a hypersonic flow

At present work the high-voltage pulse discharge and 1 MHz RF discharge have been used for the generation of the nonequilibrium conductivity in the uniform magnetic field. Characteristic current and voltage of the discharges are presented in Figure 2. The discharges have been studied without flow and in a hypersonic flow, with and without the magnetic field.

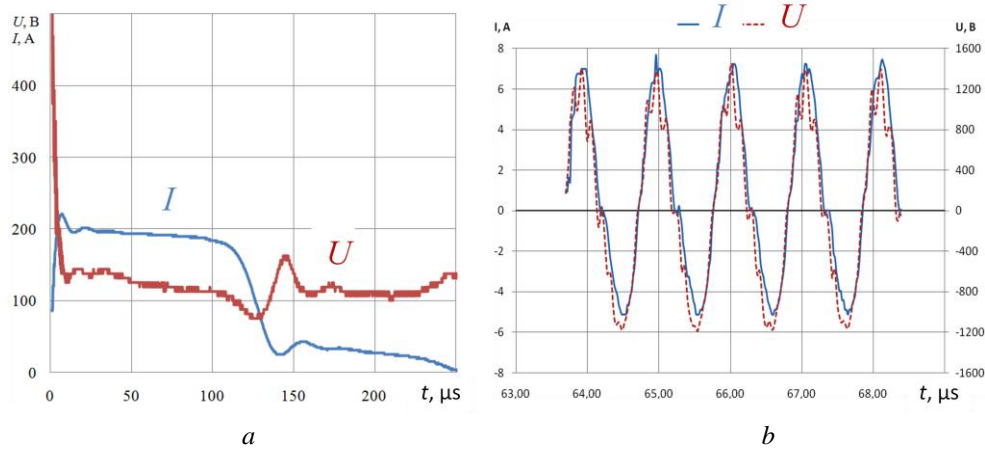


Figure 2: Current and voltage of the pulse discharge (a) and RF discharge (b)

3.1 Pulse and RF discharges initiated in the B-field direction

The **pulse discharge** initiated in the B-field direction has been studied by the schematic presented in Figure 3. The top electrode is cathode. The pulse generator has been operated in a current generator mode. The magnitude of the discharge current was about 100 A and the voltage was of 3-4 V. The voltage has been changed according to the test conditions.

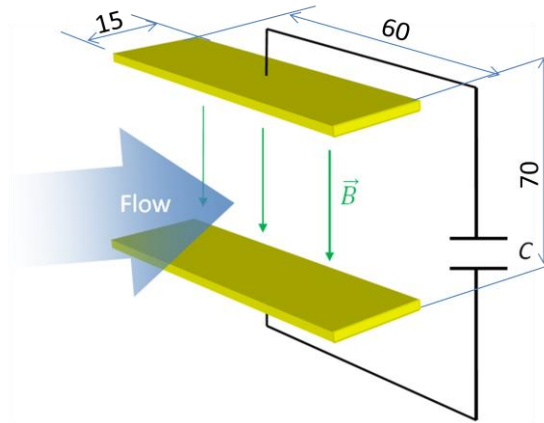


Figure 3: Test schematic

The uniform discharge occurs with the air static pressure $P_{st} = 3$ Tor without B-field. The picture stays stable with $B = 0.34$ T. But the pressure increasing to 5 Tor leads to the discharge stratification. The gas conductivity value has been estimated by the current, the voltage and geometry of luminous area and was of 0.8 S/m.

Pictures of the pulse discharge initiated in the hypersonic flow with $M = 6$, $P_{st} = 5$ Tor are presented in Figure 4. The voltage was 3 kV, the current was 8 A. The back-view is in the left side of the picture and the side-view is in the right. The hypersonic air flow blows the discharge from the electrodes (Fig. 4a). When B-field more than 0.19 T the discharge returns in the electrodes area (Fig. 4b,c) and has a rather uniform structure. Further B-field increasing leads to the discharge contraction (Fig. 4d-f).

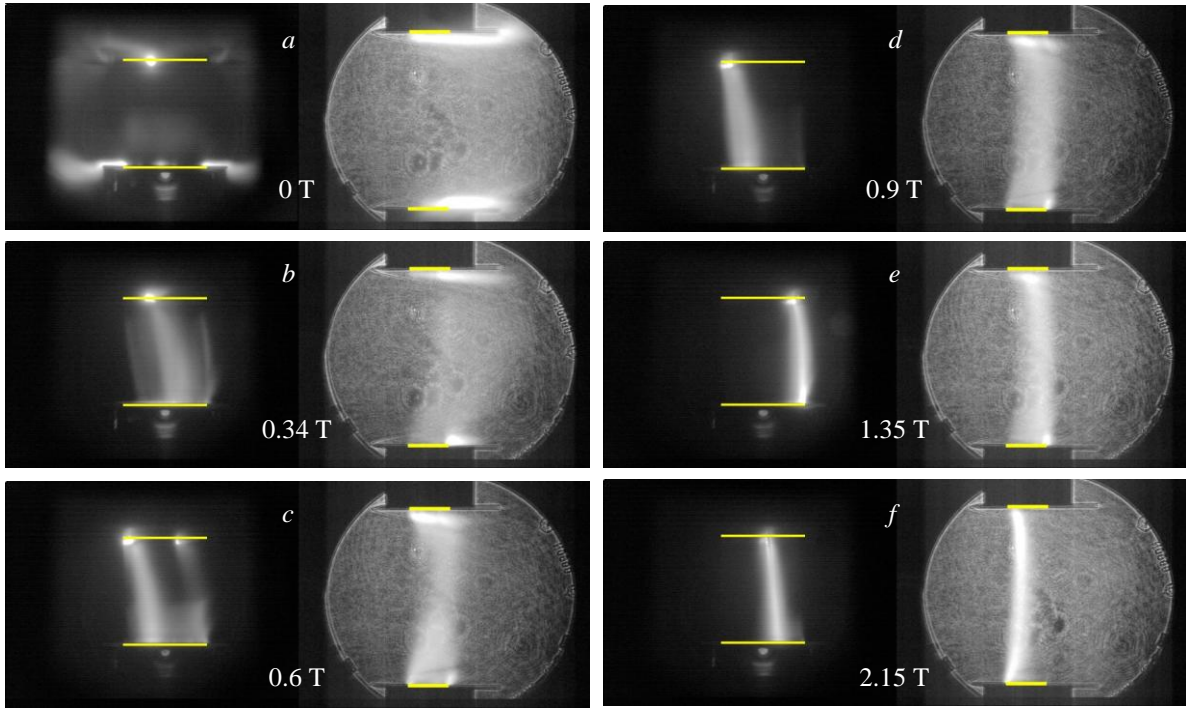


Figure 4: Discharge area in the flow and magnetic field

The voltage and the conductivity of the discharge area have been changed according to the magnitude of B-field. Dependence of the conductivity value on B-field induction is presented in Figure 5. As can be seen, the contraction of the discharge leads to the rapid increasing of the conductivity up to 10 S/m at B-field more than 2 T.

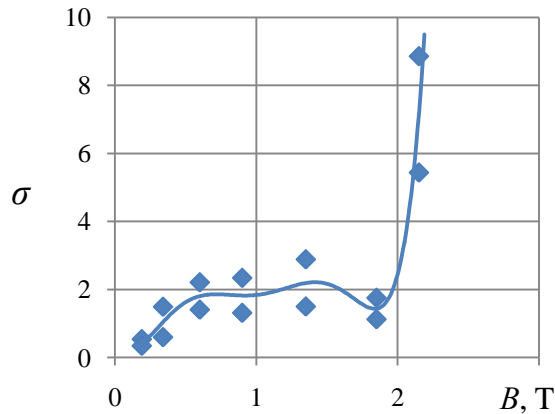


Figure 5: Conductivity vs B-field induction

The RF discharge initiated in the B-field direction has been studied under the same conditions. Flow Mach number was 6, the static pressure was 5 Tor and the B-field varied up to 2.15 T. The current was about 8 A, the voltage was about 8 kV and changed according the test conditions. Pictures of the discharge area are presented in Figure 6, where columns A and B show the RF discharge without flow (back-view and side-view respectively), columns C and D – in the hypersonic flow.

As can be seen, the discharge takes all the space between the electrodes without flow. The flow blows the discharge from the electrodes. When B-field more than 0.21 T the discharge returns in the electrodes area and has a rather uniform structure. Further B-field increasing leads to the discharge stratification.

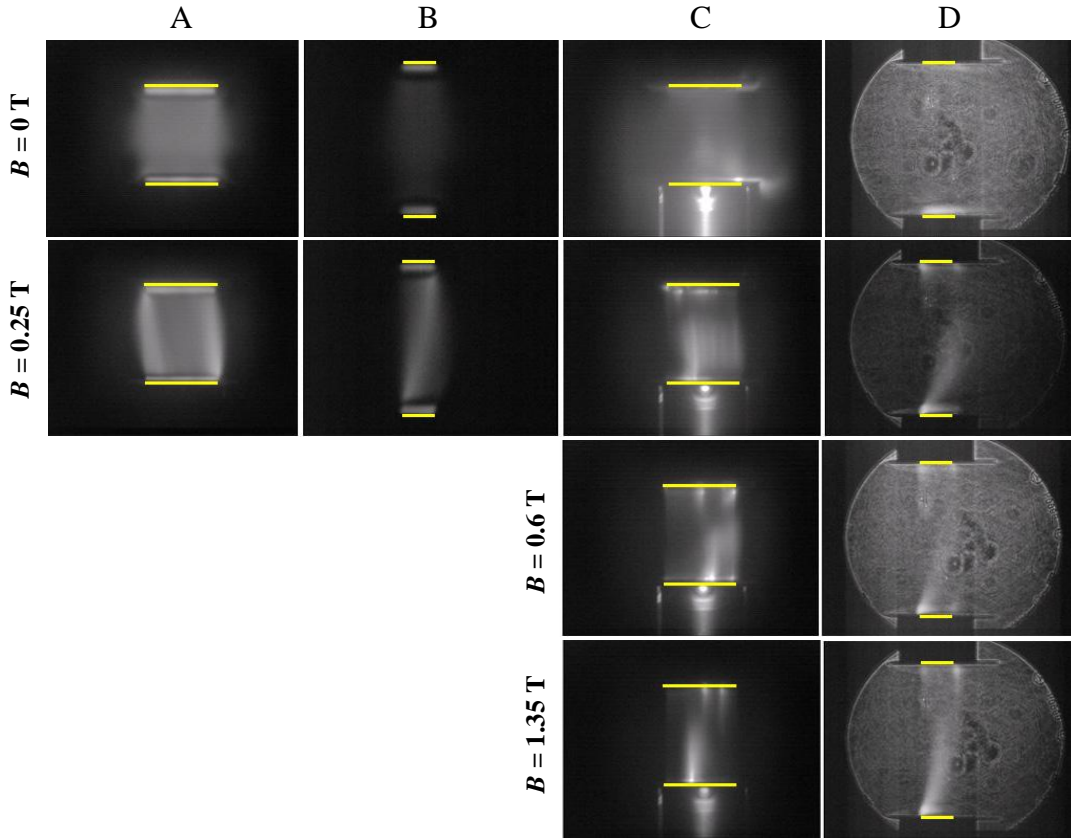


Figure 6: RF discharge in the flow and magnetic field.

The conductivity was about 0.5 S/m without flow and weakly depends on B-field increasing. The dependence of the discharge conductivity on the B-field induction in the hypersonic flow presented in Figure 7.

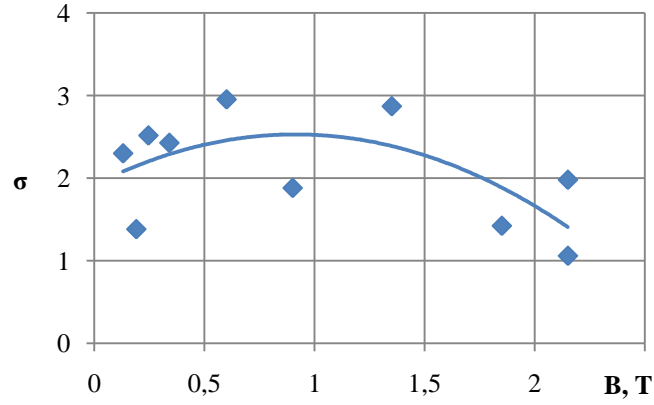


Figure 7: Conductivity vs B-field induction

3.2 Pulse and RF discharges initiated across the B-field direction

The pulse discharge initiated across the B-field direction between thin electrodes has been studied by the schematic presented in Figure 8 but without the model. The distance between the electrodes was 30 mm and the electrodes dimensions were 15×2 mm.

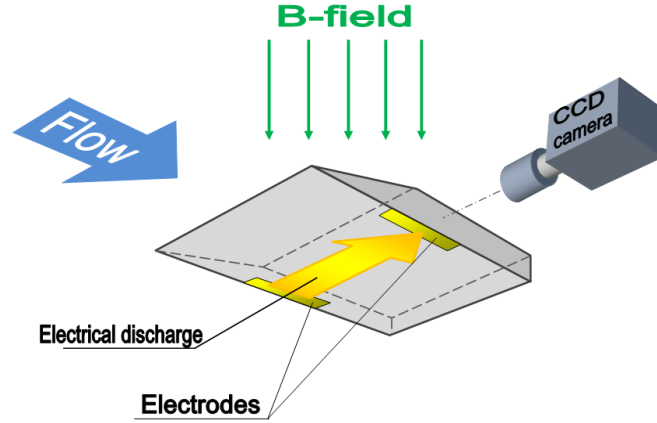
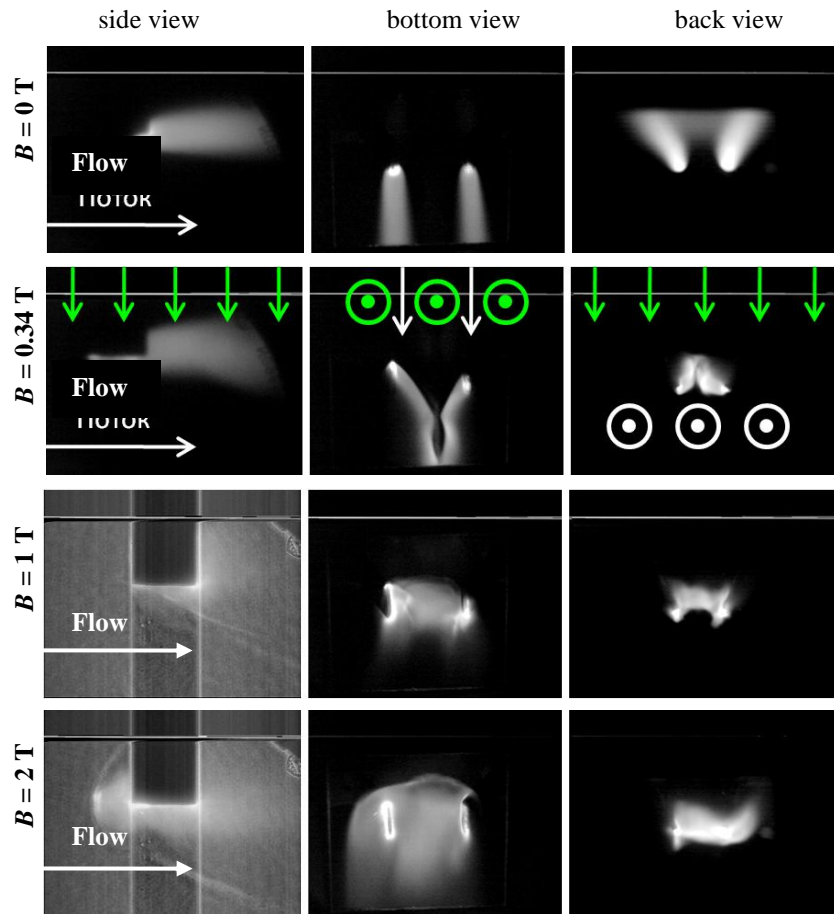


Figure 8: Test schematic.

Pictures of the flow have been taken in three directions: on march coordinate, in side view and in bottom view. Studies of the discharge without flow have been shown that the increasing pressure leads to the increasing of the discharge area, the other way B-field increasing leads to the contraction of the discharge.

Figure 9 demonstrates the discharge burning in the hypersonic flow with $M = 6$. The flow blows the discharge from the electrodes. B-field returns the discharge in the electrodes area. The discharge region generates an oblique shock wave because of significant deceleration of the flow. Further B-field increasing leads to the discharge motion upstream and to the transformation of the oblique shock wave to the detached normal shock. The dependence of the flow conductivity on B-field induction is shown in Figure 10.

Figure 9: Pulse discharge in the flow with $M = 6$

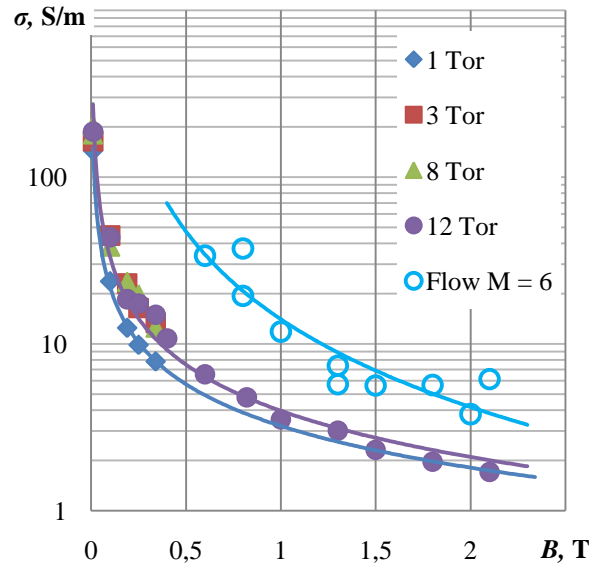


Figure 10: Conductivity vs B-field induction

The RF discharge initiated across the B-field direction between thin electrodes has been studied at the same conditions. The discharge region grows with the increasing of the pressure without flow and B-field increasing leads to the contraction of the discharge as in the case of pulse discharge burning. To organize the RF discharge in the flow has been failed. Figure 11 shows the dependence of the conductivity on the B-field induction at different air pressure.

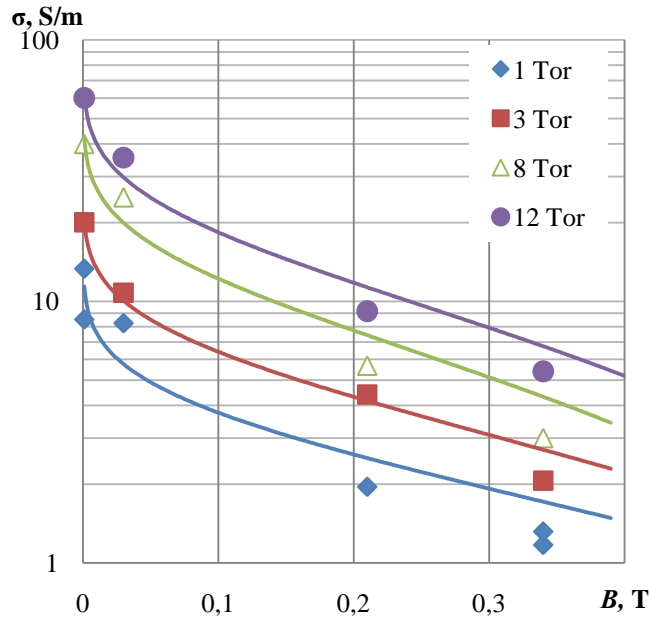


Figure 11: Conductivity vs B-field induction

4. Experimental studies of the MHD-action on a shock wave structure in a hypersonic flow

4.1 Demonstration of the MHD-parachute phenomena

In ref. [3] authors consider a concept of the MHD-parachute. The main goal is to reduce the velocity of the reentry vehicle into the upper atmosphere (where the increasing of the heat flux because of MHD-interaction is not critical) down to the values that could assure a low heat load into the dense atmosphere. It has shown that a strong MHD-interaction leads to the formation of the detached bow shock and significantly decreases the total heat flux to the

body surface. In this case the MHD interaction region greatly exceeds the middle transverse section of the body, which ensures effective braking at the low gas density in the upper atmosphere.

The concept has been studied experimentally [4] in ITAM on the MHD-test rig described above. Test schematic shown in Figure 8. MHD-interaction is provided by external pulse discharge within 120 ms. Flow parameters: Mach number is $M = 6$, the static flow pressure is of 12 Torr, the static temperature is of 270 K, the flow rate is of about 2 km/s. The wave structure of the flow has been visualized by Schlieren-technique with exposure time of 1.2 ms. The electromagnet generates an external magnetic field up to 2.3 T. The model width is 50 mm, the length is 50 mm, the sizes of each electrode are 1.5×15 mm, and the distance between the electrodes is 47 mm. The generator of the RF current operated in a current generator mode. The discharge current was held at a level of 8 A with an open circuit voltage of about 8 kV.

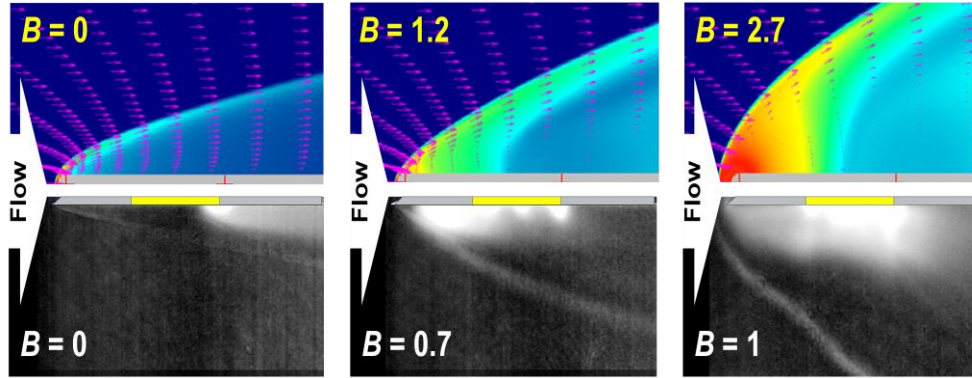


Figure 12: Comparison of numerical data (on the top) and experimental results (at the bottom)

Although the flow ionization had been achieved by electrical discharge it did not effect on a good agreement between test results and numerical data (Fig. 12) [3]. Tests have shown that the flow blows the discharge away from the model without magnetic field. The magnetic field returns the discharge in the area between the electrodes at $B = 0.19$ T. As a result of increasing of magnetic field up to $B = 0.7$ T, the discharge moves to the leading edge of the model under the ponderomotive force. The following increasing of magnetic field put forward the conductive area upstream, ahead the model, and transforms an oblique shock into the normal shock. When $B > 0.9$ T discharge region goes ahead the model on both sides of the plane, pushes away the shock wave of the model and significantly expands the area of the MHD interaction.

The model under 15 degrees angle of attack has been studying as well. Tests have shown that the effect is possible at this condition too. Figure 13 shows Shlieren-pictures of the flow at $M = 6$ with angle of attack. When $B = 0$ the flow also blows the discharge away from the surface. The increasing of magnetic field leads to the upstream movement of the discharge area that results in transformation of the oblique shock wave to the normal shock.

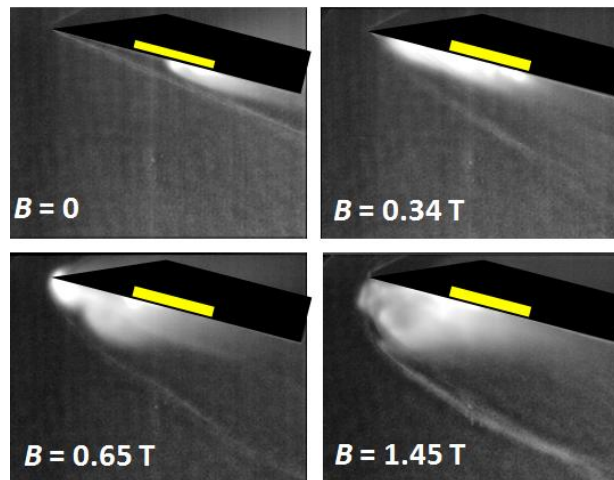


Fig. 13. Model under angle of attack of 15 degrees.

The pulsations of the discharge voltage occurred at $B > 0.7$ T, which are directly related to the bow shock pulsations. This process has been additionally investigated using high-speed camera during the first 60 μ s (two periods of voltage pulsations) at $B = 0.9$ T with zero angle of attack.

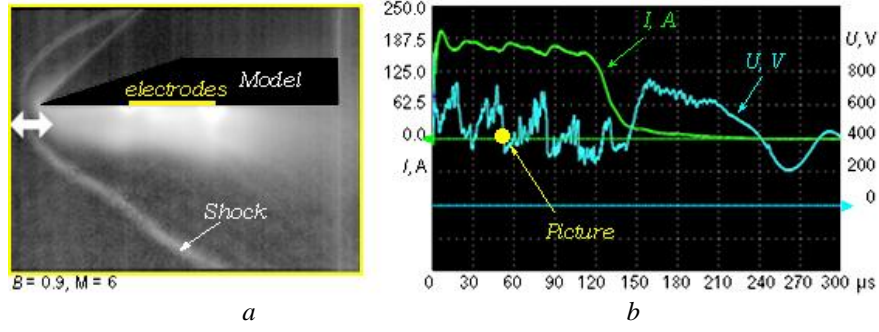


Fig. 14. Bow shock pulsations mode.

a – picture of the flow around the model, *b* – current and voltage of the discharge.

Figure 14*a* presents the picture of the flow when the bow shock went upstream from the leading edge and the typical current and voltage oscillograms of the discharge in the Figure 15*b*. We suspect that the voltage drop occurs due to bypass of the current loop at its upstream movement. Then the discharge initiates between the electrodes again and repeats the process. Obviously the discharge motion leads to the bow shock motion. This process has a periodical nature with the frequency up to 30 – 35 kHz at test conditions.

It is possible to estimate the MHD-interaction parameter knowing the current density of discharge area, B-field induction and flow parameters. We have optimized the formula of Stewart parameter to a convenient form:

$$S = \frac{I B}{b \rho_{\infty} v_{\infty}^2} \quad (1)$$

where *b* is an average height of the discharge area cross-section in a B-field direction, *I* – measured current, $\rho_{\infty} v_{\infty}^2$ – flow strength. Results of computations have shown that the bow shock pulsations occur at $0.2 < S < 0.25$. When B-field induction exceeds 2 T, the efficiency of the MHD-interaction significantly drops off at test conditions. It is happened due to destruction of the interaction area and shock wave structure of the flow. Graph of Stewart number on B-field induction is presented in Figure 15.

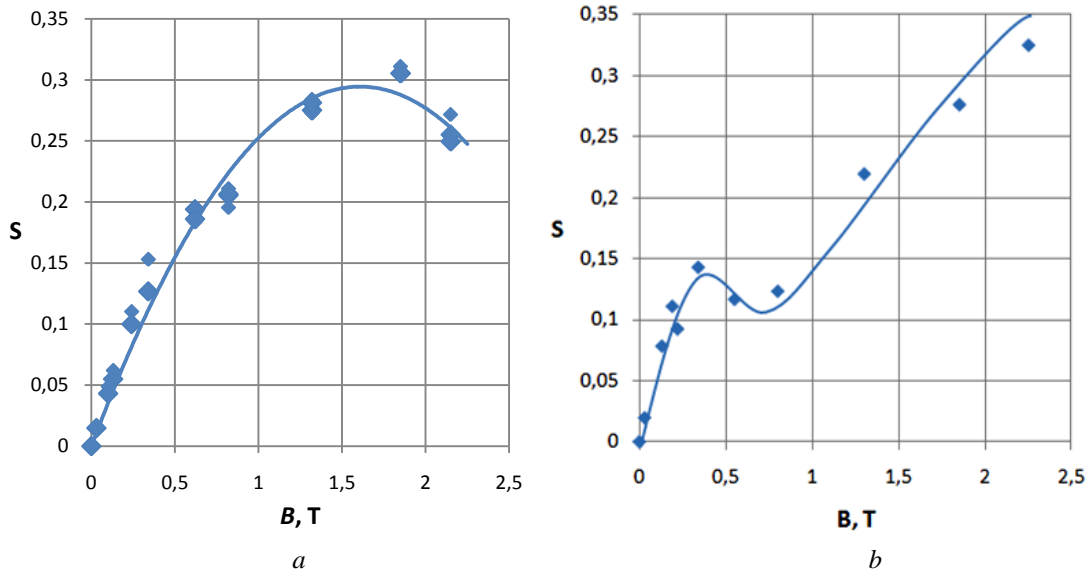


Figure 15: MHD-interaction parameter vs B-field induction.

a – model at zero angle of attack, *b* – model at 15 degrees angle of attack

4.1 Realization of the MHD-flap

Experiment study of the MHD-effect with RF-discharge was carried out at the same conditions at $M = 6, 8$. Using of the RF-discharge is rather interesting because the local conductivity area is created with practically constant resistance and electrical contact between the electrodes. The RF-oscillator and pulse discharge works in the current supply mode. The discharge frequency is of 1 MHz and the duration is of 290 μs . The current and open-circuit voltage are of 8 A and 8 kV respectively.

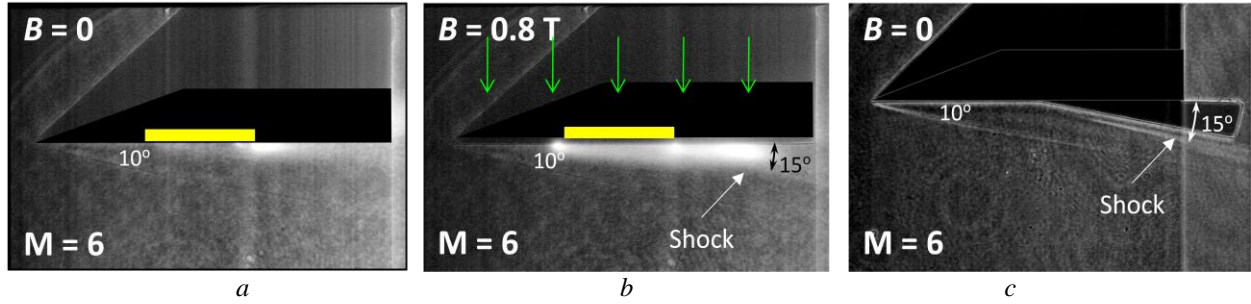


Figure 16: MHD-flap and equivalent aerodynamic configuration

While the flow blows the discharge of the plate, the magnetic field returns the discharge into the electrodes area as it shown in Figure 16b. In this case the discharge region generates a new oblique shock wave. Experimental studies have been shown that the angle of the shock is increases with the B-field respectively. When the shock wave slope angle is of 15 degrees at $B = 0.8$ T, that corresponds to the hypersonic flow near the plate with extended flap at 10 degrees (Fig. 16c). Such alteration under MHD-interaction can be interpreted as “MHD-flap”. The MHD-effect permits to generate control forces and moments on the body surface under a hypersonic flight conditions.

5. Conclusions

It has been shown experimentally that both the pulse and the RF discharge can be efficiency used for the flow ionization in the transverse B-field and for the generation of the nonequilibrium conductivity. That confirmed by the significant MHD-influence on a shock wave structure over the plate. The MHD-interaction permits to control the shock wave structure of the flow and generate control forces and moments on the surface streamlined at test conditions. In particular, a local MHD-interaction on a flat plate leads to the transformation of the attached oblique shock wave to the detached normal shock at $S > 0.2$ using the electrical pulse discharge as an ionizer. And 1 MHz RF discharge in the magnetic field leads to the generation of the new oblique shock wave near the model surface. The nature of the obtained effects planning to study in a future work devoted to the MHD flow control.

References

- [1] Fomin, V., M. Fomichev, V., P. Golovnov, I., A. Korotaeva, T., A. Pozdnyakov, G., A. Pravdin, S., S. Shashkin, A., P. Yakovlev, V., I. Study of MHD-interaction in hypersonic streams. *AIAA Paper 2004-1193*.
- [2] Pavlov, A., A. Pavlov, A., Al. Golubev, M., P. Use of AVT for gas flow visualization. *In: 14th ICMAR Conference*, 2008, Novosibirsk, Russia.
- [3] Biturin, V., A. Bocharov, A., N. MHD Parachute in ReEntry Flight Induced Electric Field Effects in Hypersonic MHD Flow. *In: 2nd International ARA Days*, October 21-23, 2008, Arcachon, France.
- [4] Fomichev, V., P. Podzin, V., E. Shevchenko, A., B. Yadrenkin, M., A. Experimental Study of the MHD-Parachute Phenomena in a Hypersonic Air Flow. *In: AIAA Hawaii Summer Conference 2011*, Honolulu, June 27-30, 2011, AIAA-2011-3462.